Surface-Initiated Growth of Thin Oxide Coatings for Li–Sulfur Battery Cathodes

*Kyu Tae Lee, Robert Black, Taeeun Yim, Xiulei Ji, and Linda F. Nazar**

1. Introduction

The challenges of exhaustion of petroleum resources and environmental pollution require development of more fuel-efficient hybrid electric vehicles (HEV), that in turn demand safe, high energy density and long-lasting rechargeable batteries as a power source.[1] A very promising candidate is the lithium-sulfur battery.[2,3] Conventional cathodes in lithium ion batteries use a lithium transition metal oxide or phosphate that operate on the basis of intercalation chemistry, and thus have an inherent limited specific capacity of between 150–200 mAh/g.[4] The sulfur cathode in the Li–S battery has an outstanding advantage of much higher specific capacity (theoretical: 1675 mAh/g) and two times larger volumetric energy density than the commercialized $LiCoO_2$-graphite system,[5–8] based on the redox couple described by the "assimilation" reaction: $S_8 + 16Li \longleftrightarrow 8Li_2S$. On the other hand, there are numerous problems with its practical use, even though the Li–S cell is very attractive as a next generation Li battery system.

Sulfur is a highly electrically insulating material. To enable reversible redox access, the sulfur (and its reduction product; Li_2S) must be in intimate contact with a conductive additive. Sulfur-carbon macro-composites can overcome this problem to a limited degree.[9–11] We have reported that nanostructured sulfur-infiltrated mesoporous carbon (CMK-3) composites dramatically improve the electrical conductivity (CMK-3/S); and demonstrate high reversible capacities between 1000–1300 mAh/g.[12,13] The carbon framework not only acts as an electronic conduit to the sulfur encapsulated within, but also functions as a electrochemical reaction chamber to confine the intermediates formed in the reaction. The latter – polysulfide anions, S_x^{n-}– that are formed on reduction of S_8 or oxidation of Li_2S, are highly soluble in the polar organic solvents used in electrolytes.[14] Without kinetic and chemical constraint, they diffuse away from the cathode and cross over to the Li anode where they are reduced to solid precipitates (Li_2S_2 and/or Li_2S). On charge, they partially reform polysulfide anions which are then redeposited on the cathode. The result is high polarization and poor coulombic efficiency.[15] Inhibition of this so-called shuttle mechanism in the nanostructured sulfur/carbon cell[12,13] is aided by hydrophilic polymer functionalization of the mesoporous carbon surface. The entrapment ensures a more complete redox process takes place, and results in enhanced utilization of the active sulfur material. Nonetheless, capacity degradation eventually occurs on repeated long-term cycling of the cell because the confinement is not 100% efficient.

Here we present a way to more fully inhibit the dissolution of polysulfides by enshrouding porous-carbon/sulfur composites with an inorganic thin film shell formed by the surface-initiated growth of oxides. In this work, we demonstrate the principle using two porous carbons; CMK-3, with a narrow small mesopore size distribution centered at 3.5 nm,[12] and a large pore SCM ("silica colloidal monolith") SCM with a large mesopore about 12 nm in diameter.[13] In order to effect production of a surface barrier without substantially increasing the polarization, the inorganic layer on the CMK-3/S or SCM/S must be very thin and homogeneous. Another critical limitation is that the coating must be processed at relatively low temperature (≤ ca. 100 °C) to prevent melting or evaporation of sulfur during the coating process.

Many methods have been reported for creating passivating layers on active electrode materials with inorganic oxides such as Al_2O_3 using sol-gel techniques, or AlF_3, in order to enhance their electrochemical performance.[16–19] Such protective layers have had an enormous impact on capacity stabilization by reducing reactivity with the electrolyte, and inhibiting dissolution of the cathode. However, these conventional sol–gel methods can be difficult to control, and utilizing them to produce an ultra-thin, homogenous coating on carbon (in contrast to lithium metal oxides) at low temperatures is challenging. Another efficient way to generate homogeneous thin layers is chemical vapour deposition (CVD), which has been used to deposit SiO_x layers on $Li[Ni_{0.8}Co_{0.2}]O_2$ at high temperatures,[20] or a related atomic layer deposition (ALD) method, a gas-phase synthesis using repetitive sequential reactions to control the thickness of the layers.[21] This method includes several steps; i) purging a reactant gas and carrier gas on the functionalized surface at high temperature (>100 °C), ii) reaction of reactants and the functional group on the surface, iii) eliminating (by evacuation) all un-reacted reactants and by-products, iv) functionalizing the surface again, v) repeating the processes in (i-iv). Here, we describe a very simple and general method using surface-initiated growth of metal oxides on functionalized particle surfaces (CMK-3/S and SCM/S) that invokes catalyzed formation of the coating in-situ. The principle of this method is similar to that of ALD, but it is much simpler and efficient.

Dr. K. T. Lee,[†] R. Black, T. Yim, X. Ji, Prof. L. F. Nazar
University of Waterloo
Department of Chemistry
Waterloo, Ontario, Canada N2L 3G1
E-mail: lfnazar@uwaterloo.ca
[†] Current Address: Ulsan National Institute of Science and Technology (UNIST), Interdisciplinary School of Green Energy, Ulsan, 689-798, South Korea

DOI: 10.1002/aenm.201200006

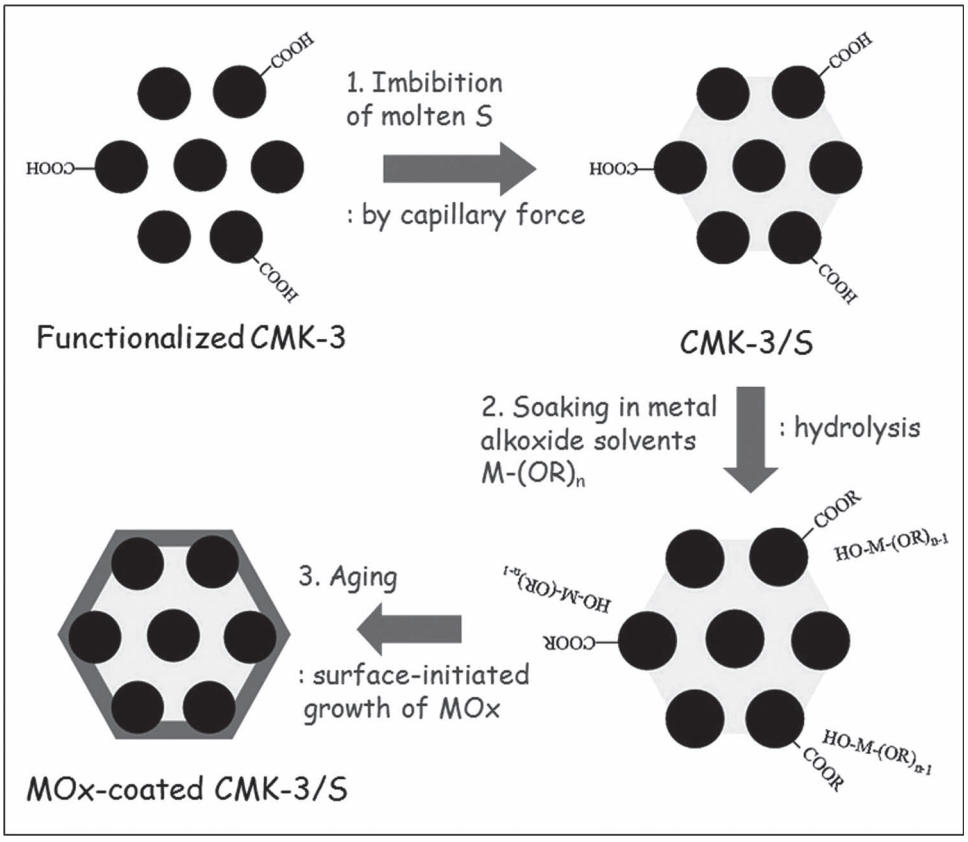

Figure 1. Schematic diagram for the synthesis of MO_x-coated CMK-3/S composites

2. Results

2.1. Silica Deposition

Figure 1 shows the proposed mechanism of the surface-initiated growth of oxides on the functionalized CMK-3/S composite. Surface derivatization of carbons is well known, and is achieved by exposure to oxidizing agents that include HNO_3, H_2SO_4, H_2O_2, permanganate, plasma, and ozone.[22,23] We treated CMK-3 in a concentrated HNO_3 solution, a process known to decorate the surface with anchors such as hydroxy (–OH), carboxyl (–COOH) and carbonyl (–C = O) groups that are necessary to tether metal ions to the surface of the carbon. Sulfur was then imbibed into CMK-3 at elevated temperature using our previously reported melt-diffusion method, to achieve a 4:6 ratio of functionalized CMK-3 (f-CMK-3) and sulfur.[12] The liquid sulfur is imbibed into the channels by capillary forces, whereupon it solidifies and shrinks to form sulfur nanofibers in intimate contact with the conductive carbon walls. Next, the f-CMK-3/S composites were soaked in neat metal alkoxide precursors (without any catalyst or solvent) to initiate the surface reaction. Two oxides (SiO_x and VO_x) were deposited on the CMK-3/S composites using tetraethyl orthosilicate (TEOS), and triisopropoxide vanadium oxide, respectively. We propose that the carboxylic groups (–COOH) on the CMK-3 react with the metal alkoxide precursors ($M\text{-}(OR)_n$), to form carboxylate ester (–COOR) and hydrolyzed metal alkoxides ($HO\text{-}M\text{-}(OR)_{n-1}$), as illustrated above in Figure 1.[24] Further hydrolysis and condensation reactions between hydrolyzed forms of metal alkoxides are propagated during aging by the evolution and consumption of H_2O. This results in a thin, homogeneous MO_x-coated CMK-3/S composite, since initial oxide deposition primarily occurs by reaction with the surface functional groups.

The powder morphologies before and after the SiO_x coating process are essentially the same. In the coated material, no visible bulk second phase is evident that would correspond to the segregation of silica (**Figure 2**a). The SEM image shows the results for 2.7 wt% silica deposition as determined by TGA analysis (Figure 2b), but no segregation was apparent even if much higher amounts of silica were deposited on the surface using longer contact times with TEOS (ie, up to 26.5 wt%). In TGA profiles, sulfur and carbons are lost under air at around 200 and 500 °C, respectively. The presence of a uniform SiO_x-coating is especially clear in the TEM images shown in **Figure 3**. Note that the filling of the pores with sulfur is evident from the decrease in contrast vis a vis CMK-3 itself, but the contrast is still noticeable in the CMK-3/S composite (Figure 3a and Figure 3b). However, the SiO_x shell on the CMK-3/S surface results in a complete lack of differentiation of the arrays of carbon and sulfur due to the mask afforded by the surface layer (Figure 3c). The presence of SiO_x surface species on the CMK-3/S was also examined using TEM, by employing EDS elemental maps (Figure 3d). The silicon, oxygen, sulfur and carbon elemental maps demonstrate that the SiO_x coating layer

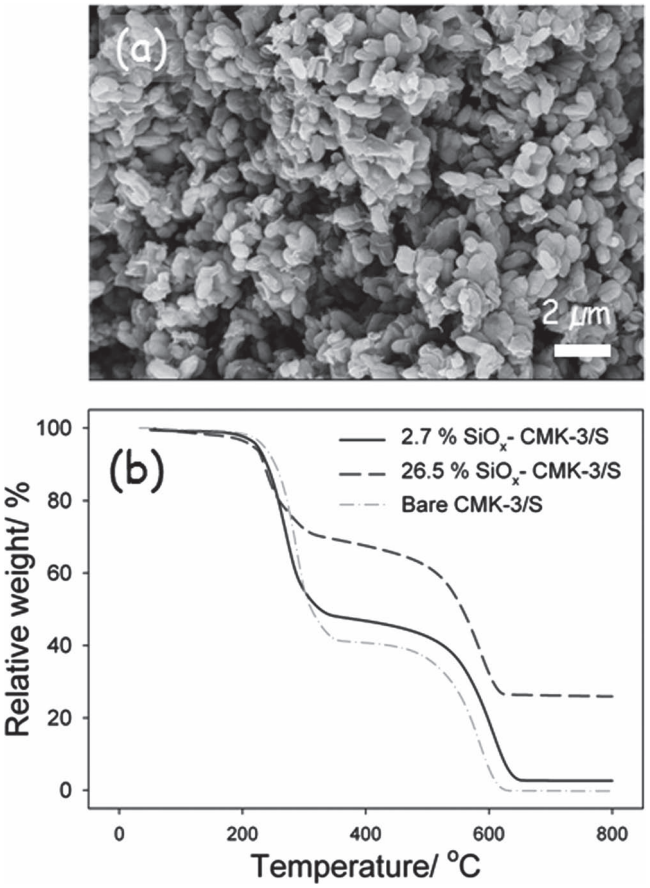

Figure 2. (a) SEM image of 2.7 wt.% SiO_x-coated CMK-3/S composites and (b) TGA profiles of SiO_x-coated and bare CMK-3/S composites.

is evenly distributed on the surface of CMK-3/S. The same process was used to coat the SiO_x onto the surface of a large pore carbon, SCM, which possesses pores that average 12 nm in diameter as discussed further below.

2.2. Vanadia Deposition

Vanadium oxide also formed a uniform coating on the surface of CMK-3/S as indicated in the FESEM images (**Figure 4**). Careful control of the deposition conditions, using contact times of vanadium alkoxide with the surface functionalized material of <1 day, resulted in a surface coating as low as 1.8 wt% as determined by TGA analysis (Figure 4a). Larger VO_x contents were possible by increasing the contact time, but they were detrimental to electrochemical performance (*vide infra*). Comparison of the carbon/sulfur array after deposition of oxide (Figure 4a) shows that, similar to the case of the SiO_x, a homogeneous thin film shell (gray arrow) covers the carbon/sulfur array. A portion of the coating has broken off, revealing the underlying carbon/sulfur array (indicated by the black arrow). The thickness is < *ca*. 5 nm, as estimated from the edge of the fractured coating in the SEM image. Nonetheless, it is difficult to distinguish between a ~5 nm oxide coating, and a monolayer of carbon rods (6 nm in thickness based on the dimension of

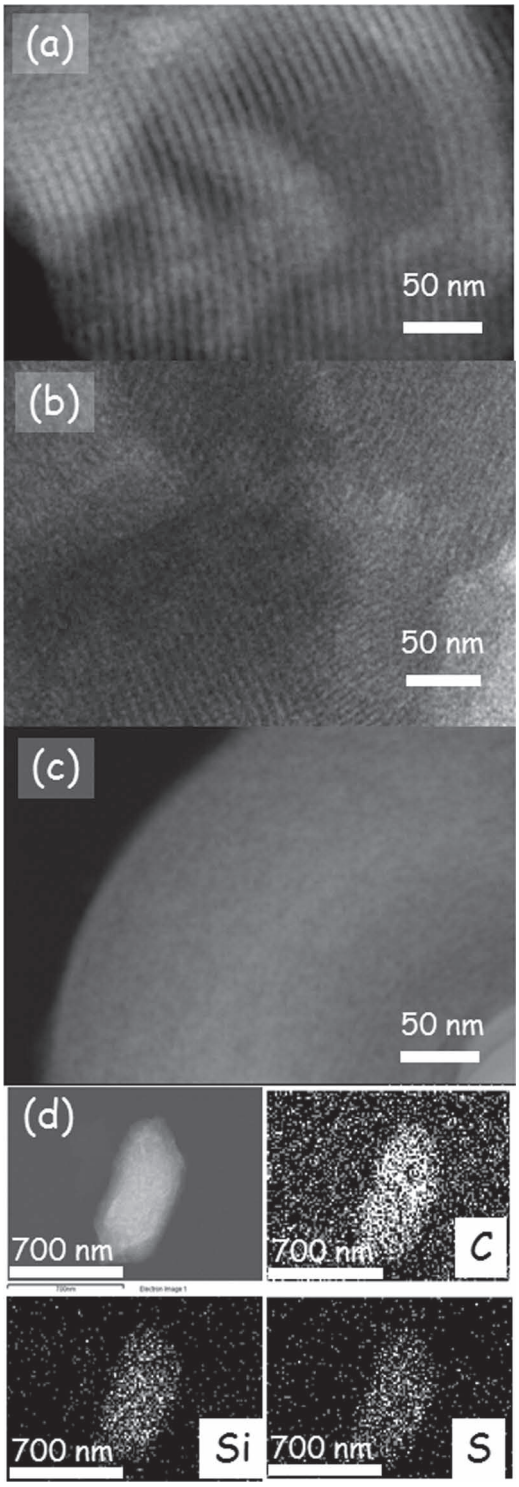

Figure 3. TEM images of (a) CMK-3, (b) CMK-3/S, (c) 26.5 wt.% SiO_x-coated CMK-3/S, and (d) EDS mapping image of 26.5 wt.% SiO_x-coated CMK-3/S showing the TEM image in the upper left hand corner, and the C, Si, and S elemental maps as indicated

the rods) with a <1 nm oxide coating. The EDS elemental maps indicated the presence of a uniform VO_x shell with retention of sulfur within the structure (Figure 4c). We note that in general,

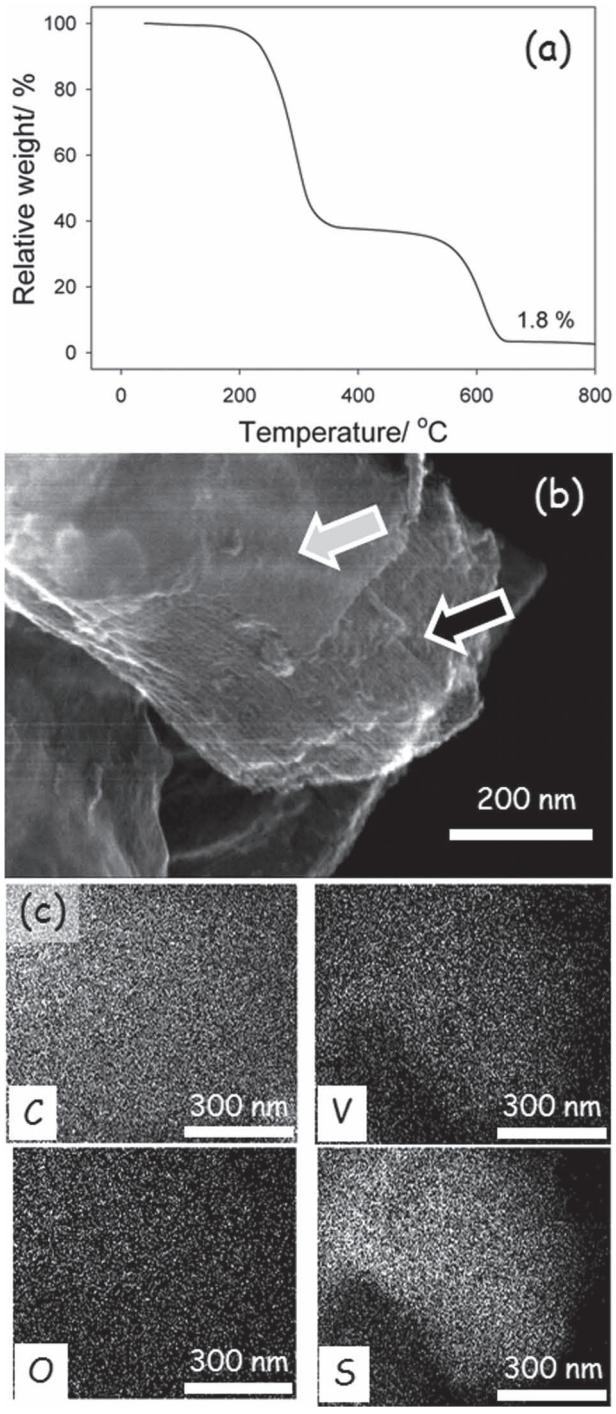

Figure 4. (a) TGA profile, (b) FESEM image and (c) EDS mapping of the VO_x-coated CMK-3/S composite showing the C, V, O and and S elemental maps as indicated.

sol-gel reactions are rapid, and proceed to completion in a few hours in the presence of a catalyst such as H_2O.[25] However, in the case of the surface-initiated sol-gel reaction on carbon, the reaction rate is quite slow and it takes from 1 day to 2 weeks to grow the layers. This slow rate, attributed to the low fraction of functional groups on the carbon surface, allows control of the layer thickness.

3. Discussion & Electrochemical Properties

3.1. CMK-3/S Coated Materials

The discharge-charge profiles of CMK-3/S and SiO_x-coated CMK-3/S at the 1st and 10th cycle are shown in **Figure 5**a at a C/10 rate. There are two plateaus in the discharge profile. The first, which contributes a minor portion to the overall capacity in the voltage window from 2.4 to 2.0 V, corresponds to the conversion from elemental sulfur (S_8) to Li polysulfide anions (Li_2S_x; where x is typically 4 to 5). The second plateau at around 2.0 V is due to the conversion of polysulfides into Li_2S_2 or Li_2S. At the 1st cycle, SiO_x-coated CMK-3/S shows larger irreversible capacity loss than CMK-3/S, and the amount of irreversible capacity loss increased as the amount of SiO_x increased. Usually, the irreversible capacity loss at the 1st cycle is caused by electrolyte decomposition on the surface of electrodes to form a solid-electrolyte interphase (SEI) layer. Therefore, the larger irreversible capacity loss is considered to be attributed to that more electrolyte decomposition occurs on the surface of SiO_x layers than the surface of CMK-3/S. The higher reactivity of SiO_x with electrolyte is ascribed by unstable SiO_x structure. SiO_x obtained from sol-gel process at room temperature in general includes alkoxide or hydroxide impurities, and thus should be heated at high temperature to form SiO_2. These impurities are electrochemically unstable, and thus it is accelerated to form SEI on the surface, resulting in larger irreversible capacity loss. Although the reversible capacity of SiO_x-coated CMK-3/S is slightly lower than that of CMK-3/S during initial cycling, the overcharge caused by the polysulfide shuttle effect which increases upon long-term cycling is largely diminished. The coulombic efficiency ($Q_{discharge}/Q_{charge}$) of the 2.7 wt% SiO_x-coated CMK-3/S at the 60th cycle is 85.8%, higher than that of the CMK-3/S without coating (80.7%). Furthermore, the SiO_x-coated CMK-3/S composites show much more stable cycling performance (Figure 5b and 5c). After 60 cycles, the reversible capacity of the 2.7 wt% SiO_x-coated CMK-3/S is 82.5% of the maximum capacity, compared to only 56.8% for CMK-3/S without any coating.

We note that the higher coulombic efficiencies and lower reversible capacities of SiO_x-coated composites go hand in hand. The SiO_x coating inhibits the dissolution of polysulfides, but it also increases the charge transfer resistance. This can be evaluated indirectly by controlling the thickness of the SiO_x shell by varying the contact time. We found that surface layers less than 1 wt% SiO_x (i.e., reaction for less than 24 hrs) were not effective at stabilizing the electrochemical properties compared to bare CMK-3/S. Conversely, thicker SiO_x coatings prepared by increasing the contact time from 4 days to two weeks (26.5wt% SiO_x, (Figure 2b), exhibit very stable coulombic efficiency but at the expense of greatly increased polarization and a decreased reversible capacity (Figure 5a). Clearly if one was able to reproducibly decrease the amount of SiO_x from 2.7 wt% to about 1%, while still retaining a very uniform thin coating, the electrochemical properties might be further improved. We note that thin SiO_2 and Li_2SiO_3 coatings prepared at high temperature on a variety of cathode materials including $LiMn_2O_4$,[26] and $LiCoO_2$,[27] used for cathode stabilization show high Li^+-ion permeability as long as the coating is relatively thin.

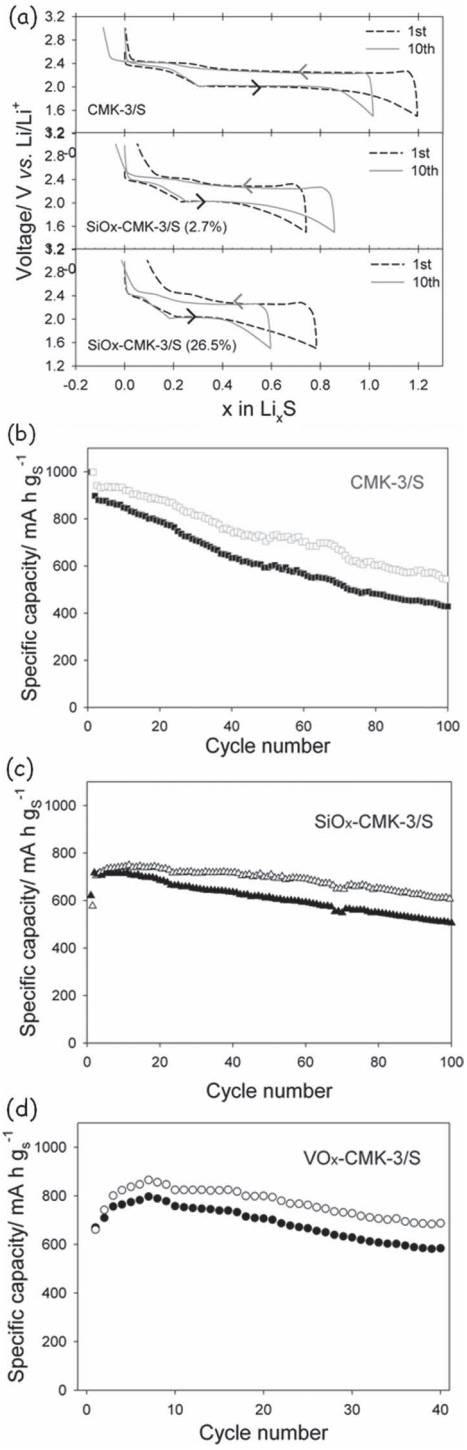

Figure 5. (a) Voltage profiles at the 1st and 10th cycle and cycling performance of (b) CMK-3/S, (c) 2.7 wt.% SiO_x-coated CMK-3/S and (d) 1.8 wt.% VO_x-coated CMK-3/S (open circle: charge, closed circle: discharge). Black and gray arrows indicate lithiation (discharge) and delithiation (charge) profiles, respectively.

Even better would be surface coatings that have the potential for both Li^+- ion and electronic conductivity. We studied vanadium oxide to explore this approach, since VO_x (ie, amorphous $V_2O_{5-\delta}$) intercalates lithium between 2.8 –2.0 V (depending on the degree of insertion) to form Li_yVO_x - a mixed ion/electron conductor. It is thus well matched to the Li/S redox potential (2.2 V *vs* Li).[28] *In-situ* transformation of the VO_x coating to Li_yVO_x is expected to first occur, followed by reaction of Li with the sulfur within the carbon composite. The discharge-charge profile of the 1.8 wt.% VO_x coated CMK-3/S composite was very similar to that of the SiO_x coated material, both on the first cycle and the 10th (Figure 5a). The capacity as a function of cycle number is shown in Figure 5d. The reversible capacity of the VO_x-coated sample (797 mAh/g) is higher than that of the 2.7 wt.% SiO_x-coated sample, possibly because of the better conductive properties of VO_x *vis a vis* SiO_x. This material also exhibits stable cycling performance which is better than the pristine material, but surprisingly it is not significantly improved vs. the 2.7 wt.% SiO_x-coated sample. We note that in both VO_x and SiO_x-coated materials, the capacity is lower on the 1st cycle, but increases quickly due to a "formation" process. This occurs after one cycle for SiO_x, and within 8 cycles for VO_x. We speculate that this may arise from partial cracking of either coating upon cycling and/or reaction with Li, that occurs more rapidly for SiO_x, and which slightly compromises the integrity of the surface. Thus, overcharge becomes evident on prolonged cycling although certainly much less so than in the unmodified case.

3.2. Large-Pore Carbon Coated Materials

Further investigations were conducted with a large-pore porous carbon (SCM) with a narrow pore size distribution centered at 12 nm, using a less viscous electrolyte optimized for high current rates that such a larger pore diameter permits. The SCM pore structure is also shown in Figure 7; more details on its preparation and pore size distribution are available elsewhere.[13] The surface coating is especially important to inhibit polysulfide dissolution in larger pore carbon systems, because diffusion is much more pronounced as we have previously noted. The f-SCM/S-SiO_x composites were synthesized by carbon functionalization, sulfur impregnation and followed by a TEOS catalyzed sol-gel reaction using the same protocol that was established for CMK-3 (see Experimental Section). After completion of the surface modification process, TG analysis (**Figure 6**a) confirmed a SiO_x coating accounting for 7.5 wt% of the total weight. TEM imaging revealed the presence of a uniform distribution of Si (**Figure 7**) suggesting that as in the case of CMK-3/S, a thin film was present on the SCM/S composites.

The electrochemical cycling performance of SCM/S and SiO_x-coated SCM/S is shown in Figure 6b at a high **1C rate** over 200 cycles. In the initial stages, the discharge capacity is mainly governed by the conductivity of the cathode composite. The SCM/S shows a higher initial discharge capacity than the SiO_x-coated SCM/S because the SiO_x is nonconductive. However, the non-coated SCM/S showed more significant capacity degradation just after the start of cycling (a drop from 1125 mAh/g to 1000 mAh/g, corresponding to a 12% capacity loss) compared to f-SCM/S with the silica coating (918.8 mAh/g to 897.4 mAh/g, 2% capacity loss). Typically, a substantial capacity drop in the first few cycles is the result of loss of sulfur in the cathode via dissolution of the initially formed polysulfide in the outermost area of the sulfur/carbon composite. The surface

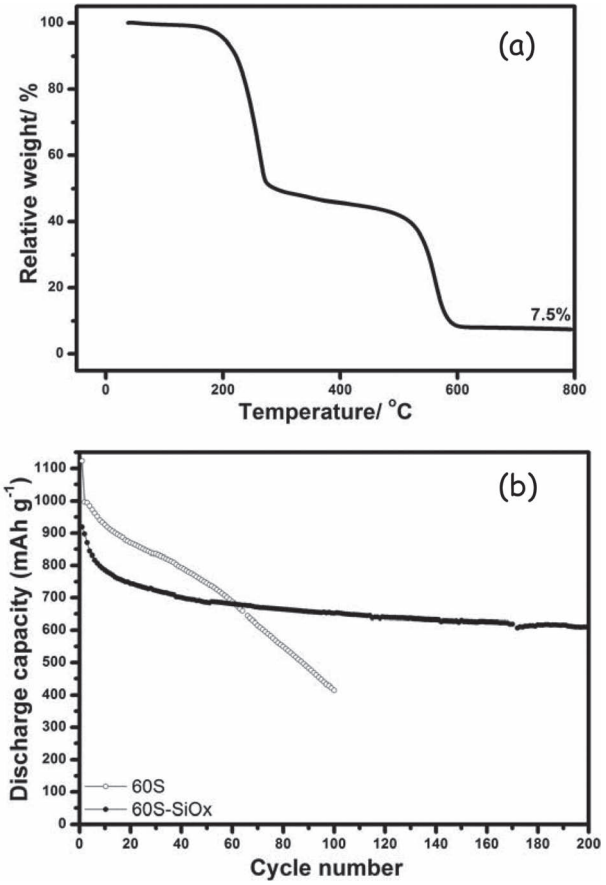

Figure 6. (a) TGA profile of the SiO_x-coated SCM/60S composite; (b) cycling performance of SCM/60S and 7.5 wt.% SiO_x-coated SCM/60S (open circle: SCM/S, closed circle: SiO_x-coated SCM/S).

nature owing to the low temperature synthesis route. This permits ingress of the electrolyte into the interior of the carbon/sulfur composites as demonstrated by the high rate behavior. The surface pore structure is impossible to quantify in the presence of the underlying imbibed sulfur, but nonetheless work is underway to optimize its properties.

4. Conclusions

In summary, we demonstrate a facile route to generate homogeneous surface layers of MO_x (M = Si, V) on mesoporous carbon-sulfur composites. The improvement of the coulombic efficiency and capacity fading of the SiO_x-coated C/S composites can be explained based on the same arguments used for hydrophilic-polymer coated CMK-3/S reported earlier.[12] Namely, the presence of an insulating coating inhibits the electrochemical reduction of polysulfides on the cathode surface that form insoluble, impermeable layers. Secondly, and probably more importantly, the SiO_x coating retards the dissolution of polysulfides. It thus alleviates the both problem of the loss of active mass, and polarization resulting from the deposition of insoluble sulfides and results in enhanced performance of the active sulfur material. The 2.7 wt.% SiO_x-coated CMK-3/S composite exhibits a reversible capacity of 718 mAh/g, and can sustain up to 82.5% of the initial reversible capacity after 60 cycles, representing almost twice the capacity retention of the pristine composite materials without the inorganic shell. Nonetheless, the reversible capacities of MO_x-coated CMK-3/S composites are reduced *vis a vis* the uncoated materials because of their increased impedance. The use of a vanadium oxide coating improved the reversible capacity compared to that of SiO_x possibly due to its conductive properties, but the cycling stability was similar. The excellent stability was attained with

SiO_x hydrophilic coating layer suppresses this to a large degree owing to its effective interaction with the hydrophilic (poly)sulfide, despite the large pore diameter of the carbon. The f-SCM/S composites showed higher discharge capacity after 60 cycles and consistently maintained much more stable cycling performance even after 100 cycles. The reversible capacity of the 7.5 wt% SiO_x-coated SCM/S is 71% of the 1st discharge capacity, compared to only 37% for SCM/S without any modification at 100 cycles. In addition, the cathode with f-SCM/S exhibited stable cycling even after 200 cycles (66% capacity retention compared to its 1st discharge capacity) and only 5% capacity loss occurred over the next 100 cycles. This demonstrates that polysulfide intermediates are effectively stored within the large mesopores even with a small fraction of hydrophilic coating on the carbon surface.

We note that the SiO_x coating prepared by this surface initiated method must possess some limited microporosity given its amorphous

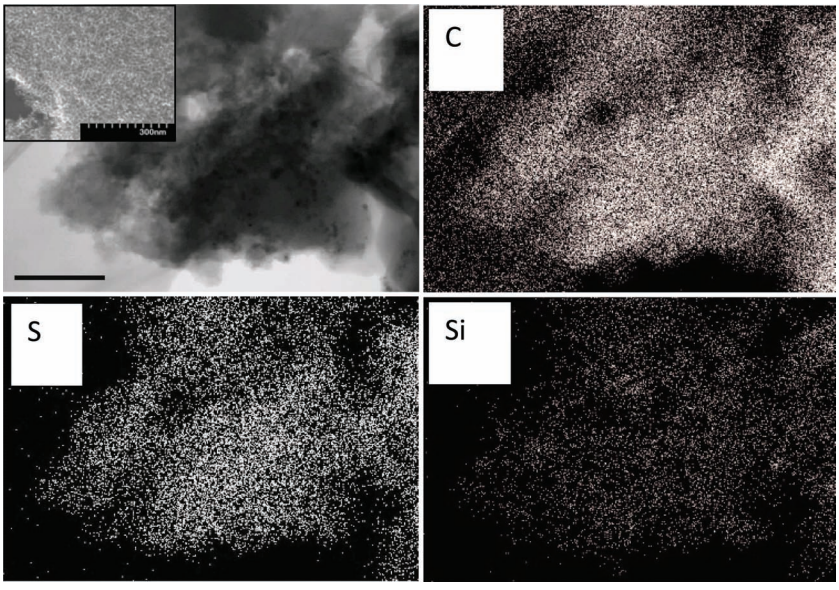

Figure 7. TEM - EDS mapping of the SiO_x-coated SCM/S composite showing the TEM image in the upper left hand corner (inset shows an FESEM image of the original SCM pore structure); the C, S and Si elemental maps as indicated.

large pore (12 nm) carbons for which the coatings were very effective for long term cycling.

This work points the way to other approaches that could utilize "flexible" hybrid inorganic-polymer coatings, for example combining polyethylene glycol (PEG) which proved very effective in initial studies;[12] polyvinyl pyrrolidone (PVP);[29] or inactive conductive inorganic coatings (such as lithium phosphorus oxynitride, LiPON) prepared at low temperature. Work is ongoing in our laboratory to establish these chemistries. To this end, we note that promising results have been very recently reported for other organic coatings alone, such as poly(3,4-ethylenedioxythiophene)-poly(styrene sulfonate) (PEDOT:PSS) on CMK-3.[30] Also, due to the flexibility of binding various MO_x coatings via the surface-initiated "atomic-layer" deposition process illustrated here, we believe that this strategy could find broad application in many areas of materials science, not only as advanced electrode material coatings in lithium secondary batteries.

5. Experimental Section

Synthesis: The CMK-3 carbon and SCM carbon were synthesized as previously reported.[11] The CMK-3/S and SCM/S nanocomposites were prepared following a melt-diffusion strategy. The mesoporous carbon (CMK-3 or SCM) and sulfur were ground together, pelletized and heated overnight. In order to allow for expansion of the pore content upon full lithiation to Li_2S, the weight ratio of carbon/sulfur was adjusted to 3:7 for normal CMK-3 and 4:6 for functionalized CMK-3 and SCM. To prepare the MO_x-coated CMK-3/S and SCM composite, CMK-3 and SCM were first functionalized with carboxylic groups by oxidization treatment in concentrated HNO_3 solution (70%, Aldrich) for half an hour at 80 °C, prior to incorporation of the sulfur by melt-imbibition. The f-CMK-3/S and f-SCM/S composites were then soaked in either neat TEOS (Aldrich), or triisopropoxide vanadium oxide (for f-CMK-3/S) (Aldrich), and kept in a glove box under Ar atmosphere at room temperature for a specific duration (ranging from 1 day for 1.8 wt.% VO_x-coated CMK-3/S, 4 days for 2.7 wt.% SiO_x-coated CMK-3/S and 7.5 wt.% SiO_x-coated SCM/S to 2 weeks for the 26.5 wt.% SiO_x-coated CMK-3/S materials). In an average experiment, 100 mg of carbon/sulfur were combined with 0.1 ml of TEOS, using 1 drop of concentrated HCl (37%, Aldrich) to catalyze the reaction. The MO_x-coated CMK-3/S and SCM/S composites were collected by filtration and dried at 90 °C. We note that sulfur is somewhat soluble in the metal alkoxide precursors, and thus the minimum amount of precursor should be used.

Characterization: The morphologies of the MO_x-coated composites were examined by transmission electron microscopy (TEM) using a Hitachi HD-2000 STEM. Scanning electron microscopy (SEM) was carried out on a LEO 1530 field emission SEM and the SEM mode of a Hitachi HD-2000 STEM. Thermogravimetric analysis (TGA) was carried out under air using a TA instrument SDT Q600.

Electrochemistry: Positive electrodes were comprised of 84 wt% MO_x-coated CMK-3/S composite, 8 wt% Super-S carbon and 8 wt% poly(vinylidene fluoride) (PVdF) binder. The cathode materials were slurry-cast from cyclopentanone onto a carbon coated aluminum current collector (Intelicoat). The electrolyte was composed of a 1.0 M $LiPF_6$ solution in ethyl methyl sulfone (EMSF) for f-CMK-3/S composites and a 1.0 M LiTFSI solution in 1,2-dimethoxyetahne (DME) and 1,3-dioxolane (DOL) (1:1 volume ratio) for f-SCM/S composites. According to the active mass loading (~1.2 mg/cm^2), the equivalent current density for the C/10 rate (167 mA/g) rate is 0.2 mA/cm^2 and 2 mA/cm^2 for the C rate (1672 mA/g). A rate of nC corresponds to a discharge (or charge) of 2 Li per sulfur (Li_2S) in 1/n hr. Lithium metal was used as the counter electrode.

Acknowledgements

NSERC is gratefully acknowledged for financial support. We thank Dr. Neil Coombs, University of Toronto, for help with acquisition of the TEM and SEM images.

Received: January 23, 2012
Revised: March 9, 2012
Published online: August 27, 2012

[1] P. G. Bruce, *Solid State Ionics* **2008**, *179*, 752.
[2] R. D. Rauh, K. M. Abraham, G. F. Pearson, J. K. Surprenant, S. B. Brummer, *J. Electrochem. Soc.* **1979**, *126*, 523.
[3] J. Shim, K. A. Striebel, E. J. Cairns, *J. Electrochem. Soc.* **2002**, *149*, A1321.
[4] K. Kang, Y. S. Meng, J. Bréger, C. P. Grey, G. Ceder, *Science* **2006**, *311*, 977.
[5] H. Yamin, A. Gorenshtein, J. Penciner, Y. Sternberg, E. Peled, *J. Electrochem. Soc.* **1988**, *135*, 1045.
[6] P. G. Bruce, S. A. Freunberger, L. J. Hardwick, J. M. Tarascon, *Nat. Mater.* **2011**, *11*, 19.
[7] J. R. Akridge, Y. V. Mikhaylik, N. White, *Solid State Ionics* **2004**, *175*, 243.
[8] S.-E. Cheon, S.-S. Choi, J.-S. Han, Y.-S. Choi, B.-H. Jung, H. S. Lim, *J. Electrochem. Soc.* **2004**, *151*, A2067.
[9] J. Wang, S. Y. Chew, Z. W. Zhao, S. Ashraf, D. Wexler, J. Chen, S. H. Ng, S. L. Chou, H. K. Liu, *Carbon* **2008**, *46*, 229.
[10] W. Zheng, Y. W. Liu, X. G. Hu, C. F. Zhang, *Electrochim. Acta* **2006**, *51*, 1330.
[11] J. Wang, J. Yang, C. Wan, K. Du, J. Xie, N. Xu, *Adv. Funct. Mater.* **2003**, *13*, 487.
[12] X. Ji, K. T. Lee, L. F. Nazar, *Nat. Mater.* **2009**, *8*, 500.
[13] X. Ji, S. Evers, R. Black, L. F. Nazar, *Nature Comm.* **2011**, **2**, 325–331
[14] R. D. Rauh, F. S. Shuker, J. M. Marston, S. B. Brummer, *J. Inorg. Nucl. Chem.* **1977**, *39*, 1761.
[15] S.-E. Cheon, K.-S. Ko, J.-H. Cho, S.-W. Kim, E.-Y. Chin, H.-T. Kim, *J. Electrochem. Soc.* **2003**, *150*, A800.
[16] J. Cho, Y. J. Kim, T.-J. Kim, B. Park, *Angew. Chem. Int. Ed.* **2001**, *40*, 3367; M. G. Kim, J. Cho, *J. Mater. Chem.* **2008**, *18*, 5880.
[17] Y. G. Guo, Y. S. Hu, W. Sigle, J. Maier, *Adv. Mater.* **2007**, *19*, 2087.
[18] N. Ohta, K. Takada, L. Zhang, R. Ma, M. Osada, T. Sasaki, *Adv. Mater.* **2006**, *18*, 2226.
[19] J. Cho, *J. Mater. Chem.* **2008**, *18*, 2257.
[20] H. Omanda, T. Brousse, C. Marhic, D. M. Schleich, *J. Electrochem. Soc.* **2004**, *151*, A922.
[21] M.-G. Willinger, G. Neri, E. Rauwel, A. Bonavita, G. Micali, N. Pinna, *Nano Lett.* **2008**, *8*, 4201; Y. S. Jung, A. S. Cavvanagh, A. C. Dillon, M. D. Groner, S. M. George, S.-H. Lee, *J. Electrochem. Soc.* **2010**, *157*, A75.
[22] A. Stein, Z. Wang, M. A. Fierke, *Adv. Mater.* **2009**, *21*, 265.
[23] H. Huang, L. F. Nazar, *Angew. Chem. Int. Ed.* **2001**, *40*, 3880.
[24] E. J. A. Pope, J. D. Mackenzie, *J. Non-Cryst. Solids* **1986**, *87*, 185.
[25] C. J. Brinker, G. W. Scherer, in *Sol-Gel Science: The Physics and Chemistry of Sol-Gel Processing*, Academic Press, California **1990**.
[26] J.-S Kim, C. S. Johnson, J. T. Vaughey, S. A. Hackney, K. A. Walz, W. A. Zeltner, M. Anderson, M. M. Thackeray, *J. Electrochem. Soc.* **2004**, *151*, A1755.
[27] Z. Chen, J. R. Dahn, *Electrochem. Solid-State Lett.* **2003**, *6*, A221; A. Sakuda, H. Kitaura, A. Hayashi, K. Tadanaga, M. Tatsumisago, *Electrochem. Solid-State Lett* **2008**, *11*, A1.
[28] G. Sudant, E. Baudrin, B. Dunn, J.-M. Tarascon, *J. Electrochem. Soc.* **2004**, *151*, A666.
[29] S. Lim, J. Cho, *Chem. Commun.* **2008**, 4472-4474.
[30] Y. Yang, G. Yu, J. J. Cha, M. Vosgueritchian, Y. Yao, Z. Bao, Y. Cui, *ACS Nano* **2011**, *5*, 9187.